Available online at www.sciencedirect.com
ScienceDirect
Journal of Power Sources 167 (2007) 223–227
JOURNAL OF POWER SOURCES
www.elsevier.com/locate/jpowsour

Short communication

A low-temperature reaction route to high rate and high capacity $LiNi_{0.5}Mn_{1.5}O_4$

Haisheng Fang, Liping Li, Guangshe Li *

State Key Lab of Structural Chemistry, Fujian Institute of Research on the Structure of Matter and Graduate School of Chinese Academy of Sciences, Fuzhou 350002, PR China

Received 12 December 2006; received in revised form 6 February 2007; accepted 8 February 2007
Available online 17 February 2007

Abstract

New applications of lithium ion batteries in hybrid electric vehicles require high electrochemical performance such as improved power density. High crystalline submicron-size $LiNi_{0.5}Mn_{1.5}O_4$ with high capacity and high rate capability was explored in this work through a low-temperature solid-state reaction route. Samples were characterized by thermal gravimetric analysis (TGA), X-ray diffraction (XRD), transmission electron microscopy (TEM), Fourier transform infrared spectroscopy (FTIR), and cell measurements. It is found that $LiNi_{0.5}Mn_{1.5}O_4$ thus obtained has a cubic spinel structure, which can be indexed in a space group of *Fd3m* with a disordering distribution of Ni. The particle size is about 200 nm. Electrochemical tests demonstrated that the as-prepared $LiNi_{0.5}Mn_{1.5}O_4$ possesses high capacity and excellent rate capability. When discharged at a rate as high as of 8C, the as-prepared $LiNi_{0.5}Mn_{1.5}O_4$ powders can still deliver a capacity of 110 mAh g^{-1}, which shows to be a potential cathode material for high power batteries.

Keywords: Lithium ion batteries; Cathode; $LiNi_{0.5}Mn_{1.5}O_4$; High voltage; Rate capability

1. Introduction

High energy and high power lithium ion batteries are increasingly demanded due to their applications in hybrid electric vehicles, portable power tools and many power supplies. Cathode materials are the key component of the lithium ion batteries that directly determines the power density. Transition metal substituted spinel materials, $LiM_xMn_{2-x}O_4$ (M = Cr, Co, Fe, Ni, Cu), are the well-known cathode materials that can show extensive charge/discharge performance at high voltage [1–5], and hence have been widely studied for advanced lithium ion batteries. Among all these spinel oxide materials, $LiNi_{0.5}Mn_{1.5}O_4$ exhibits good electrochemical performance with a single plateau at around 4.7 V [6–8].

For all functional materials, their properties were greatly influenced by the synthesis methods. Many preparation methods have been investigated with an aim to achieve high capacity $LiNi_{0.5}Mn_{1.5}O_4$ [6–20], however, the capacity of the products ever reported is usually unsatisfactory in particular when discharged at a high rate [9,12,13,17–20]. To meet high power demands of lithium ion batteries in new applications, the rate capability of $LiNi_{0.5}Mn_{1.5}O_4$ has to be significantly improved. There are two main frequently employed strategies: one is to increase the intrinsic electronic conductivity by microstructure controlling [17–20], the other is to enhance lithium ion transport by reducing the bulk diffusion length, which can be achieved by utilization of nanostructured materials [12,21–25]. Even so, only few reports were announced to achieve the desired capacity and rate capability of $LiNi_{0.5}Mn_{1.5}O_4$ [24,25]. For instance, Kunduraci et al. [24] adopted a complex Pechini process and prepared high power nanostructured $LiNi_{0.5}Mn_{1.5}O_4$ at a temperature above 700 °C, but whether the cost of this synthesis is viable for practical application may be an issue. Caballero et al. reported a simple mechanical activation-assisted method for the preparation of nanocrystalline $LiNi_{0.5}Mn_{1.5}O_4$ with improved rate capability, while the capacity at low rates was less than 100 mAh g^{-1} which is far from the theoretical capacity of 146.7 mAh g^{-1} [23]. Their later report showed that enhancement of the capacity to about 120 mAh g^{-1} needed extra polymer addition and a high-temperature calcination at 800 °C,

* Corresponding author. Tel.: +86 591 83702122.
E-mail address: guangshe@fjirsm.ac.cn (G. Li).

0378-7753/$ – see front matter © 2007 Elsevier B.V. All rights reserved.
doi:10.1016/j.jpowsour.2007.02.015

nevertheless such synthesis conditions unavoidably raised the cost of production and led to the presence of undesired impurity in the final product [25]. On the other hand, although nanostructure materials would enhance the rate capability of the battery, the use of nanocrystalline form of cathode materials leads to greater side-reactions with the electrolyte, and ultimately more safety problems (one of the most critical issues for lithium batteries) and poor calendar life, especially for high-voltage cathode materials such as $LiNi_{0.5}Mn_{1.5}O_4$.

Owing to the problems mentioned above, exploration and development of simple and cheap preparation routes which can produce large (e.g., submicron) $LiNi_{0.5}Mn_{1.5}O_4$ particles with high capacity and high rate capability is of paramount importance for practical application. To this end, synthesis of pure phase, high crystallinity, and disordered structure $LiNi_{0.5}Mn_{1.5}O_4$ particularly in a facile way is a critical aspect but meets great challenges. The primary reason is closely related to the difficulties in single-phase synthesis of $LiNi_{0.5}Mn_{1.5}O_4$ by traditional preparation methods [4,6,9], in which high calcination temperature (>700 °C) generally used would result in the presence of undesired impurities such as NiO or $Li_xNi_{1-x}O$ in the final product, and these impurities may, to a great extent, deteriorate the electrochemical performance of $LiNi_{0.5}Mn_{1.5}O_4$, while the alternative low-temperature methods that usually produce materials of low crystallinity are also disadvantageous to the electrochemical performance [11].

In this work, we reported on a facile reaction route that yielded high crystalline, single phase and disordered structure $LiNi_{0.5}Mn_{1.5}O_4$ of a submicron-size at low temperatures, without the use of any mechanical activation or extra polymer. The $LiNi_{0.5}Mn_{1.5}O_4$ powders thus obtained by this method showed high capacity and excellent rate capability.

2. Experimental

Appropriate amounts of chemicals $LiCl{\cdot}H_2O$, $NiCl_2{\cdot}6H_2O$, and $MnCl_2{\cdot}4H_2O$ were thoroughly mixed. Subsequently, a 20 wt% excess of oxalic acid was added to the mixture, which was ground for about 0.5 h to ensure complete reaction. The obtained mixture was dried in air at 120 °C and was taken as a precursor. The precursor was calcined at 550 °C in air for 10 h, and then the final products were obtained.

Powder XRD patterns of the product were recorded on apparatus (DMAX2500, Rigaku) at room temperature using Cu Kα radiation to identify the crystalline phase. The lattice parameter was refined using Retica Rietveld program with peak positions that are calibrated by internal standard of silicon (99.9% pure). The chemical compositions of the resulting material were measured using an inductively coupled plasma spectrometer (ICP, Ultima2, Jobin Yvon, France). The size and morphology of the product were observed by a transmission electron microscopy (TEM, 200 kV, JEOL, JEM2010, Japan). Fourier transform infrared spectrum (FTIR) of the product was carried out with a Perkin-Elmer IR spectrophotometer using KBr pellet technique. TGA of the precursor was performed with a TA instrument (Netzsch thermoanalyzer STA449C) at a heating rate of 15 °C min^{-1} in a constant flow of extra dry air.

Electrochemical characterizations of the product were performed using CR2025 coin-type cell. For cathode fabrication, the as-prepared powders were mixed with 20 wt% of carbon black and 10 wt% of polyvinylidene fluoride in *N*-methyl pyrrolidinone until a slurry was formed. Then, the blended slurries were pasted onto an aluminum current collector, and the electrode was dried at 100 °C for 10 h in vacuum. The test cell consisted of the cathode and lithium foil anode which were separated by a porous polypropylene film and electrolyte of 1 M $LiPF_6$ in EC:EMC:DMC (1:1:1 in volume). The assembly of the cells was carried out in a dry Ar-filled glove box. The cells were charged and discharged over a voltage range of 3.5–5 V versus Li/Li^+ electrode at room temperature.

3. Results and discussion

We first studied the preparation of pure phase $LiNi_{0.5}Mn_{1.5}O_4$ via a low-temperature solid-state route. When starting materials, $LiCl{\cdot}H_2O$, $NiCl_2{\cdot}6H_2O$ and $MnCl_2{\cdot}4H_2O$ were fully mixed with oxalic acid in a mortar, a slurry-like precursor was gradually formed, and an acid mist of HCl was emitted during the grinding process, which resulted from the metathesis reactions between the chlorides and oxalic acid [26]. The precursor may experience a reaction as described below:

$$2LiCl{\cdot}H_2O + NiCl_2{\cdot}6H_2O + MnCl_2{\cdot}4H_2O + 3H_2C_2O_4{\cdot}2H_2O \rightarrow Li_2C_2O_4 + NiC_2O_4{\cdot}2H_2O + MnC_2O_4{\cdot}2H_2O + 6HCl\uparrow + 14H_2O$$

Since the reactions were performed at room temperature, the precursor may contain plenty of nanosized oxalate compounds [26]. It is well-known that oxalate compounds often have low decomposition temperature, thus it is highly possible to synthesize $LiNi_{0.5}Mn_{1.5}O_4$ by simply calcining the precursor at low temperatures.

The thermal evolution of the precursor was monitored by TGA. As indicated in Fig. 1, four mass losses were generally observed. Mass losses below 430 °C are associated with the water release and pyrolysis of the organic compounds, while

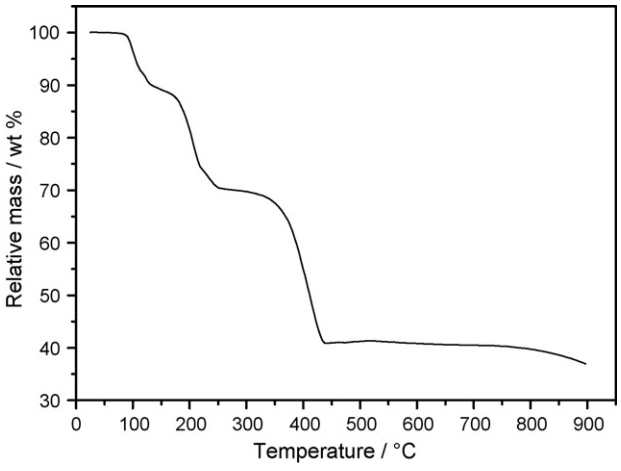

Fig. 1. TG curve of the precursor of $LiNi_{0.5}Mn_{1.5}O_4$ measured in air.

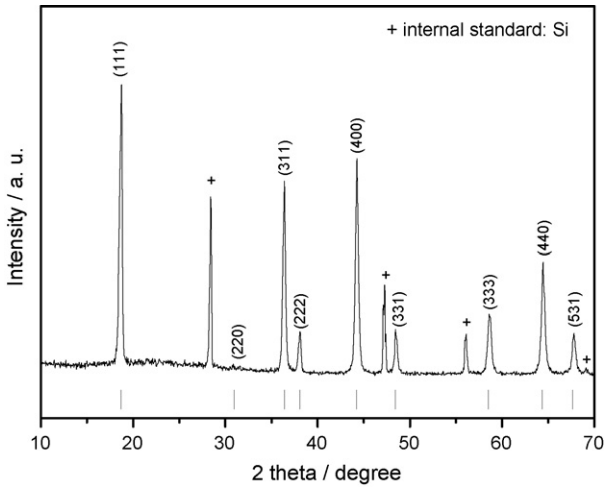

Fig. 2. Powder X-ray diffraction pattern of the as-prepared $LiNi_{0.5}Mn_{1.5}O_4$.

no mass loss was observed between 430 °C and 700 °C, which indicates that oxalate compounds and excess oxalic acid have been decomposed completely below 430 °C. However, when the temperature increased up to 700 °C, a fourth mass loss occurred, which is likely caused by oxygen loss [12]. In combination with the results reported by Zhong et al. [4], this oxygen loss should come from decomposition of $LiNi_{0.5}Mn_{1.5}O_4$. From the TGA results, we selected a moderate temperature of 550 °C to prepare pure $LiNi_{0.5}Mn_{1.5}O_4$.

Fig. 2 shows the XRD pattern of the sample synthesized at 550 °C. It is seen that all diffraction peaks were ascribed to a cubic spinel structure with a space group of *Fd*3*m*, indicating the formation of a single-phase $LiNi_{0.5}Mn_{1.5}O_4$. The chemical compositions of the sample were determined to be $Li_{1.02}Ni_{0.50}Mn_{1.49}O_4$ by ICP analysis, which are much closer to the nominal ones. The lattice parameter of the as-prepared $LiNi_{0.5}Mn_{1.5}O_4$ was calculated to be $a = 8.164$ Å. It is interesting that this low-temperature preparation route also ensures well crystallization of $LiNi_{0.5}Mn_{1.5}O_4$ powders as proved by the extensive XRD peaks. Fig. 3 shows the TEM image of the as-prepared sample. It can be seen that the particle size was about 200 nm, and shaped in a polyhedral morphology. Based on the previous literatures [6,9,11,13,14], it is noted that such a morphology of $LiNi_{0.5}Mn_{1.5}O_4$ was hardly achieved unless it was calcined at a high temperature above 800 °C. The significantly reduced sintering temperature reported in this work is likely beneficial to the utilization of nanosize precursor.

Depending on Ni ordering in the lattice, $LiNi_{0.5}Mn_{1.5}O_4$ shows two different space groups, *Fd*3*m* or $P4_332$ [10,20,27]. The structural difference between these two space groups is hardly to be distinguished by X-ray diffraction because of the similar scattering factors of Ni and Mn. Simple IR spectroscopy has proved to be an effective technique in qualitatively resolving the cation ordering [24,28,29]. Characteristic infrared vibration bands of the M–O bonds of the sample between 700 cm^{-1} and 400 cm^{-1} were used to examine the Ni ordering in $LiNi_{0.5}Mn_{1.5}O_4$. As indicated by the IR spectrum in Fig. 4, sample obtained in this work showed two bands at 623 cm^{-1} and 480 cm^{-1} which are more intensive than those at 587 cm^{-1}

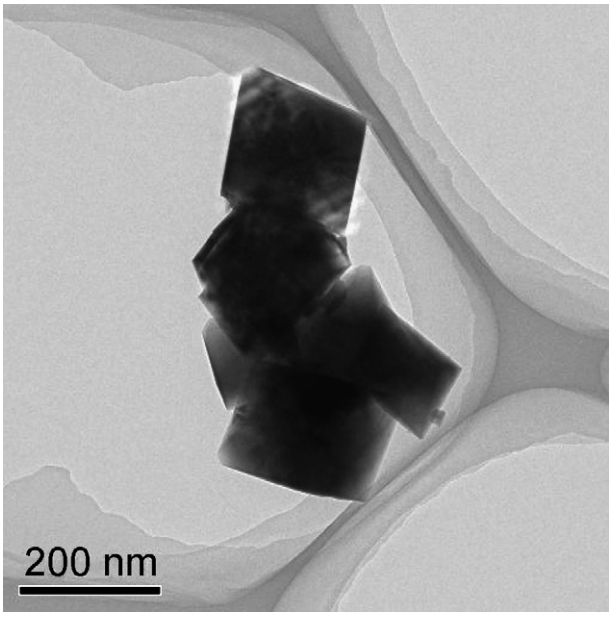

Fig. 3. Transmission electron micrograph of the as-prepared $LiNi_{0.5}Mn_{1.5}O_4$.

and 470 cm^{-1}, respectively. Such a special feature indicates a disordered structure of space group of *Fd*3*m* [24]. In addition, two bands occurred at 650 cm^{-1} and 428 cm^{-1} for $P4_332$ phase were absent or undefined in our spectrum, which further proves a disordering distribution of Ni in the structure of $LiNi_{0.5}Mn_{1.5}O_4$. No vibration bands were observed at about 3000 cm^{-1} or 1500–1550 cm^{-1} (not shown), which excludes the presence of trace impurities such as oxalate compound and Li_2CO_3 in the final product.

Many literatures have demonstrated that pure phase $LiNi_{0.5}Mn_{1.5}O_4$ with a disordering configuration is favorable to electrochemical performance improvement [4,13,20,27]. Electrochemical properties of $LiNi_{0.5}Mn_{1.5}O_4$ are evaluated using 2025 coin-type cell. Representative charge–discharge curves of $LiNi_{0.5}Mn_{1.5}O_4$ are shown in Fig. 5. The cells were cycled at two different current densities of 20 mA g^{-1} and 160 mA g^{-1}

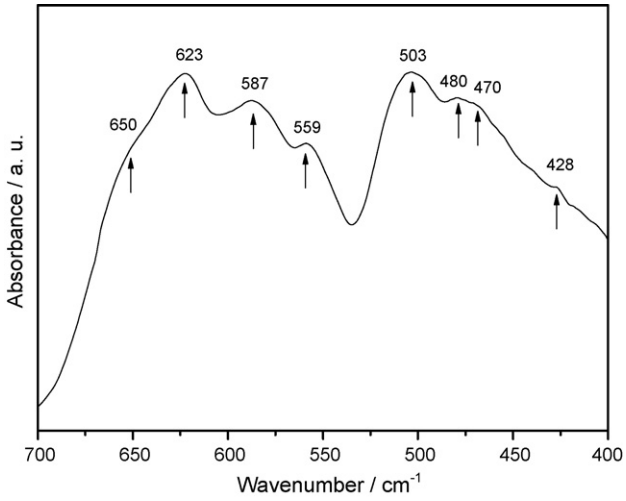

Fig. 4. IR spectrum of the as-prepared $LiNi_{0.5}Mn_{1.5}O_4$.

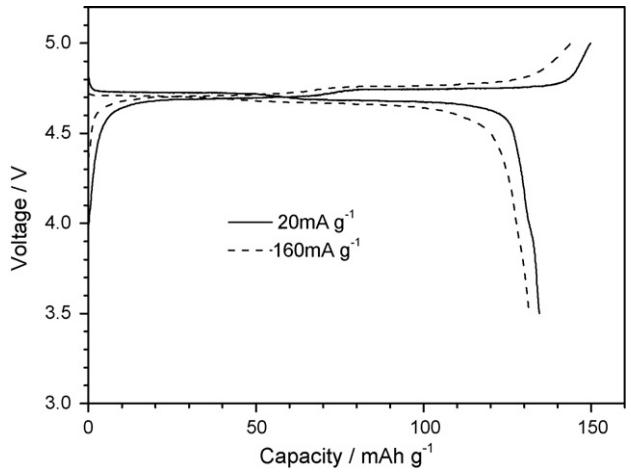

Fig. 5. Charge–discharge curves of the as-prepared $LiNi_{0.5}Mn_{1.5}O_4$ cycled at current densities of 20 mA g^{-1} (solid line) and 160 mA g^{-1} (dash line).

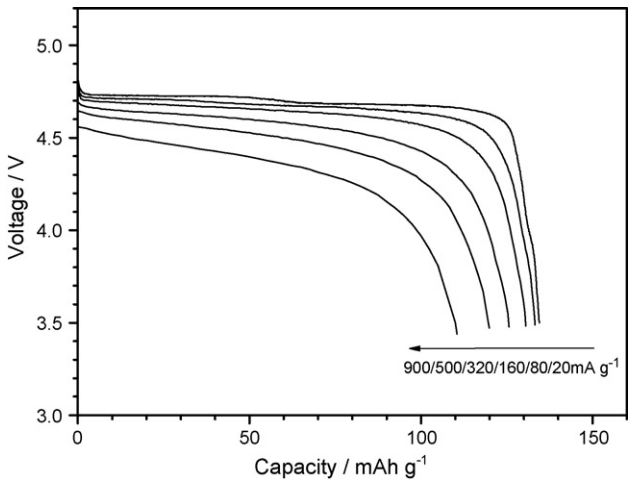

Fig. 6. Discharge curves of the as-prepared $LiNi_{0.5}Mn_{1.5}O_4$ at various current densities. In the rate test, the cell was charged at a current density of 20 mA g^{-1} to 5 V and discharged at different current densities to 3.5 V. 900 mA g^{-1} corresponds to 8C (discharge in 7.5 min).

between 3.5 V and 5 V, respectively. The charge–discharge curves of $LiNi_{0.5}Mn_{1.5}O_4$ exhibited voltage plateaus at about 4.7 V, which is attributed to the Ni^{2+}/Ni^{4+} redox couple [4]; meanwhile, both charge and discharge voltage plateau consisted of two close but distinct plateaus at around 4.7 V. It is well recognized [20,27] that $LiNi_{0.5}Mn_{1.5}O_4$ with a disordered structure (*Fd*3*m*) would show two obvious voltage plateaus at around 4.7 V while that with an ordered structure ($P4_332$) give a flat voltage profile at around 4.7 V. Therefore, the observation of two distinct plateaus at about 4.7 V in Fig. 5 confirms the disorder structure of $LiNi_{0.5}Mn_{1.5}O_4$, in consistent with our IR analysis. Mn^{3+}/Mn^{4+} redox couple can give a 4.1 V plateau, which is however absent in Fig. 5, which demonstrates a single-phase structure of $LiNi_{0.5}Mn_{1.5}O_4$. When cycled at a current density of 20 mA g^{-1}, the cell delivers a reversible capacity of 134 mAh g^{-1} which is about 91% of the theoretical capacity (146.7 mAh g^{-1}). The 1st cycle Coulombic efficiency is 75%, which progressively increases to 93% in the following cycles. The low Coulombic efficiency is mainly due to electrolyte decomposition at high voltage, just like what have taken place in many high-voltage cathode materials [4,9,30]. The capacity of $LiNi_{0.5}Mn_{1.5}O_4$ decreased while the voltage gap between charge and discharge plateau increased with the current density increasing from 20 mA g^{-1} to 160 mA g^{-1}, but these changes are still tiny. It is noted that the capacity of $LiNi_{0.5}Mn_{1.5}O_4$ synthesized in this work is much higher than that prepared by Caballero et al. [23] who had used inorganic acetates as the starting materials. Consequently, the synthesis parameters could play a key role in determining the electrochemical performance of $LiNi_{0.5}Mn_{1.5}O_4$. Following this idea, we compared the electrochemical performance of the as-prepared $LiNi_{0.5}Mn_{1.5}O_4$ with that synthesized by the present route using acetate as starting materials. We found that the capacity using acetate as starting materials is <100 mAh g^{-1}, which is almost the same as that reported by Caballero et al. [23], but is much smaller than that of this work. Therefore, the route described here is beneficial to the synthesis of $LiNi_{0.5}Mn_{1.5}O_4$ for high capacity.

Fig. 6 presents the rate capability of the as-prepared $LiNi_{0.5}Mn_{1.5}O_4$. The cell was charged at a current density of 20 mA g^{-1} to 5 V and discharged at different current densities to 3.5 V. It is clear that the as-prepared $LiNi_{0.5}Mn_{1.5}O_4$ exhibits high rate capability. Although the discharge plateau gradually shifted towards lower voltage and the discharge capacity decreased with increasing discharge current density, but these changes are much smaller as compared to those reported in literatures [9,12,13,17–20]. Even discharged at a current density of 900 mA g^{-1} (equal to 8C rate: discharge in 7.5 min), the as-prepared $LiNi_{0.5}Mn_{1.5}O_4$ still retained a capacity of 110 mAh g^{-1} which is 82% of that discharged at a current density of 20 mA g^{-1}. These results are comparable to one of the best results published for this material by Kunduraci et al. [24]. In addition, the cell retrieved its capacity when a low current density of 20 mA g^{-1} was applied after completion of the high-rates test. All these results demonstrate that the as-prepared $LiNi_{0.5}Mn_{1.5}O_4$ possesses excellent rate capability and high capacity, which could be attributed to the pure phase, high crystallinity, and disordered configuration of $LiNi_{0.5}Mn_{1.5}O_4$. Moreover, the present preparation method provides superior cost performance when comparing with those reported in literatures [24,25].

4. Conclusions

This work reports on a low-temperature solid-state route to single-phase $LiNi_{0.5}Mn_{1.5}O_4$ with a disorder occupation of Ni ion. Sample characterizations indicated that the as-prepared $LiNi_{0.5}Mn_{1.5}O_4$ was achieved to show a dimension of about 200 nm. The electrochemical performance measurements demonstrated that the as-prepared $LiNi_{0.5}Mn_{1.5}O_4$ powders have much improved capacity and excellent rate capability in comparison with those prepared by other methods. The discharge capacity reached up to 134 mAh g^{-1} at a current density

of 20 mA g^{-1}, while it retained as high as 110 mAh g^{-1} even at a high current density of 900 mA g^{-1}.

Acknowledgments

This work was financially supported by NSFC under the contract (No. 20671092), Science and Technology Program from Fujian Province (No. 2005HZ01-1 and 2006H0040), Directional program and a grant from Hundreds Youth Talents Program of CAS (Li GS).

References

[1] C. Sigala, D. Guyomard, A. Verbaere, Y. Piffard, M. Tournoux, Solid State Ionics 81 (1995) 167.
[2] H. Kawai, M. Nagata, H. Tukamoto, A.R. West, J. Mater. Chem. 8 (1998) 837.
[3] T. Ohzuku, S. Takeda, M. Iwanaga, J. Power Sources 81–82 (1999) 90.
[4] Q. Zhong, A. Bonakdarpour, M. Zhang, Y. Gao, J.R. Dahn, J. Electrochem. Soc. 144 (1997) 205.
[5] Y. Ein-Eli, W.F. Howard Jr., J. Electrochem. Soc. 144 (1997) L205.
[6] Y.S. Lee, Y.-K. Sun, S. Ota, T. Miyashita, M. Yoshio, Electrochem. Commun. 4 (2002) 989.
[7] H.S. Fang, Z.X. Wang, X.H. Li, H.J. Guo, W.J. Peng, J. Power Sources 153 (2006) 174.
[8] T. Ohzuku, K. Ariyoshi, S. Yamamoto, J. Ceram. Soc. Jpn. 110 (2002) 501.
[9] X. Wu, S.B. Kim, J. Power Sources 109 (2002) 53.
[10] Y. Idemoto, H. Narai, N. Koura, J. Power Sources 119–121 (2003) 125.
[11] J.H. Kim, S.T. Myung, Y.K. Sun, Electrochim. Acta 49 (2004) 219.
[12] M.G. Lazarraga, L. Pascual, H. Gadjov, D. Kovacheva, K. Petrov, J.M. Amarilla, R.M. Rojas, M.A. Martin-Luengo, J.M. Rojo, J. Mater. Chem. 14 (2004) 1640.
[13] S.H. Park, Y.K. Sun, Electrochim. Acta 50 (2004) 431.
[14] S.H. Park, S.W. Oh, S.T. Myung, Y.C. Kang, Y.K. Sun, Solid State Ionics 176 (2005) 481.
[15] L. Wen, Q. Lu, G.X. Xu, Electrochim. Acta 51 (2005) 4388.
[16] H.Y. Xu, S. Xie, N. Ding, B.L. Liu, Y. Shang, C.H. Chen, Electrochim. Acta 51 (2005) 4352.
[17] S.H. Park, S.W. Oh, S.T. Myung, Y.K. Sun, Electrochem. Solid-State Lett. 7 (2004) A451.
[18] J.H. Kim, S.T. Myung, C.S. Yoon, I.H. Oh, Y.K. Sun, J. Electrochem. Soc. 155 (2004) A1911.
[19] S.W. Oh, S.H. Park, J.H. Kim, Y.C. Bae, Y.K. Sun, J. Power Sources 157 (2006) 464.
[20] J.H. Kim, S.T. Myung, C.S. Yoon, S.G. Kang, Y.K. Sun, Chem. Mater. 16 (2004) 906.
[21] D. Kovacheva, B. Markovsky, G. Salitra, Y. Talyosef, M. Gorova, E. Levi, M. Riboch, H.J. Kim, D. Aurbach, Electrochim. Acta 50 (2005) 5553.
[22] J.C. Arrebola, A. Caballero, L. Hernan, J. Morales, Electrochem. Solid-State Lett. 8 (2005) A641.
[23] A. Caballero, M. Cruz, L. Hernan, M. Melero, J. Morales, E.R. Castellon, J. Power Sources 150 (2005) 192.
[24] M. Kunduraci, J.F. Al-Sharab, G.G. Amatucci, Chem. Mater. 18 (2006) 3585.
[25] J.C. Arrebola, A. Caballero, M. Cruz, L. Hernan, J. Morales, E.R. Castellon, Adv. Funct. Mater. 16 (2006) 1904.
[26] X.R. Ye, D.Z. Jia, J.Q. Yu, X.Q. Xin, Z. Xue, Adv. Mater. 11 (1999) 941.
[27] K. Takahashi, M. Saitoh, M. Sano, M. Fujita, K. Kifune, J. Electrochem. Soc. 151 (2004) A173.
[28] J. Preudhomme, Ann. Chim. 9 (1974) 31.
[29] R. Alcantara, M. Jaraba, P. Lavela, J.L. Trado, E. Zhecheva, R. Stoyanova, Chem. Mater. 16 (2004) 1573.
[30] S.T. Myung, S. Komaba, N. Kumagai, H. Yashiro, H.T. Chung, T.-H. Cho, Electrochim. Acta 47 (2002) 2543.